Granular Matter (2017) 19:24
DOI 10.1007/s10035-017-0709-6

ORIGINAL PAPER

Micromechanical origin of angle of repose in granular materials

Bei-Bing Dai[1] · **Jun Yang**[2] · **Cui-Ying Zhou**[1]

Received: 16 December 2016 / Published online: 10 March 2017

Abstract We present in this paper a numerical study of sandpile formation and angle of repose by considering the effect of particle shape. We analyze the micromechanical responses of sandpiles, which are crucial to the exploration of origin of angle of repose. The results show that the principal anisotropy directions of contact orientations for the left and right parts of sandpiles deviate increasingly away from the vertical direction as the particle shape becomes more irregular, and that the summation of their deviation angle $\Delta\phi_n$ relative to the vertical direction with angle of repose α , is approximately a constant regardless of the effect of particle shape. We find that the principal anisotropy directions of particle orientations for the left and right parts of sandpiles rotate as the irregularity of particle shape varies, and tend to reach a compromise state and to lie in the common horizontal direction at a characteristic aspect ratio AR = 0.6. We reveal that the mobilization of arching effect depends primarily on the inclined propagation of strong force chains. We also establish a relationship between the direction where the most intense arching phenomenon takes place and the principal anisotropy directions characterizing the distribution of microstructures and inter-particle force network.

Keywords Angle of repose · Particle shape · Discrete element method · Arching · Force chain · Fabric anisotropy

✉ Bei-Bing Dai
beibing_dai@yahoo.com

[1] School of Engineering, Sun Yat-sen University, Guangzhou, China

[2] Department of Civil Engineering, The University of Hong Kong, Hong Kong, China

1 Introduction

When sand particles are poured from a point source onto a horizontal plane, a conical pile with a constant slope will form, with the slope angle termed "angle of repose". Beyond this characteristic angle the sandpile surface becomes unstable and avalanches are desired to occur. The understanding of the formation of sandpiles (i.e. the origin of angle of repose) is of fundamental significance to the solution of a number of practical issues ranging from landslides and avalanches in civil and geological engineering communities to powder packing in industrial processes such as pharmaceutical production.

The previous experimental investigations indicated that a local pressure dip can be consistently observed under the apex of the pile [1–5], which is an important observation that is connected with the formation of granular piles. In these studies, a kind of stress-sensitive mat such as elastomeric substrate [1] and carbon paper [3] was used to measure the distribution of normal stress underneath the pile, while this experimental means is unable to offer insights into the micromechanical response in the pile, which is also of great importance for the understanding of sandpile formation. Alternatively, Geng et al. [6], Zuriguel et al. [7], Zuriguel and Mullin [8] and Zhang et al. [9] utilized photo-elastic disks to construct piles, and examined the particle arrangement and force chain propagation in the granular pile. Although the photo-elastic testing permits a direct visualization of particle arrangements and interactions as well as propagation paths of force chains, it is only a semi-quantitative method which cannot provide a complete quantitative description of force chains on the basis of both orientations and magnitudes of force vectors [10].

Some researchers have proposed a series of theoretical models to study the complex force network in the pile and

to explain the origin of angle of repose. Liu et al. [11] and Coppersmith et al. [12] proposed the alleged "q-model" to account for the propagation and distribution of force chains in the pile which was described by a regular lattice of particles of mass unity. But, the q-model cannot reproduce the central pressure dip at the bottom [13,14]. Bouchaud et al. [15] and Wittmer et al. [16,17] pursued a continuum-mechanical description of sandpiles by bringing forward the "FPA" model, in which the directions of principal stress axes in the sandpile are assumed to be fixed. This assumption has specified the propagation means of stresses in the pile and reflected intuitively the inherent arching effect, contributing to a successful reproduction of the macroscopic responses such as pressure dip. In addition, Alonso et al. [18] and Herrmann [19] put forward a simple lattice model, in which the angle of repose is interpreted as the state of a complete devil's staircase, and derived an analytical expression to calculate the angle of repose by taking into account the impact of various microscale factors such as particle shape and surface roughness, etc. Other researchers have also done similar theoretical analyses to interpret the formation of sandpiles [20,21].

Such theoretical studies employed analytical models to shed light on some interesting phenomena observed in sandpiles, such as arching and pressure dip, and the majority of these studies used a continuum-mechanical approach to explain the angle of repose and related phenomena. Nevertheless the sandpile formation originates from the discrete nature of granular media [22–24], and relies on the micromechanical responses of granular system. Owing to the discrete nature, the basic particle attributes such as particle shape and inter-particle friction play a crucial role in both macroscopic and microscopic responses of sandpiles.

The grain-scale modelling such as molecular dynamics (MD) and discrete element method (DEM) has been used to explore the origin of angle of repose. Lee and Herrmann [25], Luding [26], Zhou et al. [27] and Goldenberg and Goldhirsch [28] performed the MD or DEM simulations to investigate the effect of inter-particle friction on the angle of repose. Liffman et al. [29] and Li et al. [30] used idealized spherical particles to mimic the sandpile formation and scrutinize the force distribution in or underneath the pile. Alternatively using irregular-shaped particles to build up numerical models, Matuttis [31], Matuttis et al. [32], Zhou and Ooi [33] and Zhou et al. [34] studied the effect of particle shape on the formation of sandpiles. The numerical modelling has, to some extent, provided a fundamental understanding into the mechanism underlying the formation of sandpiles, but few studies have been done to probe an effective relationship between angle of repose and micromechanical indices characterizing the microstructures and inter-particle force network. Therefore the principal mechanism behind the formation of sandpiles remains unclear, and no conclusive answer has been achieved yet regarding the origin of angle of repose.

This study aims to find out the micromechanical origin of angle of repose by a DEM analysis. The effect of particle shape on the angle of repose has been discussed, with the sandpiles created with clumped particles of different shapes. We have devoted particular attention to a complete quantitative analysis of the microstructures as well as the propagation and distribution of force chains in the sandpile. We have also made an effort to explore a quantitative relation of the angle of repose and its related phenomena with the micromechanical indices, such that the angle of repose is interpreted at a microscopic level.

2 Numerical implementation

We used the DEM program PFC2D [35] to mimic the formation of sandpiles. Figure 1 shows the six particle shapes considered in this study, including the disk-shaped particle (Fig. 1a), elongated-shaped particle (Fig. 1b–e), and

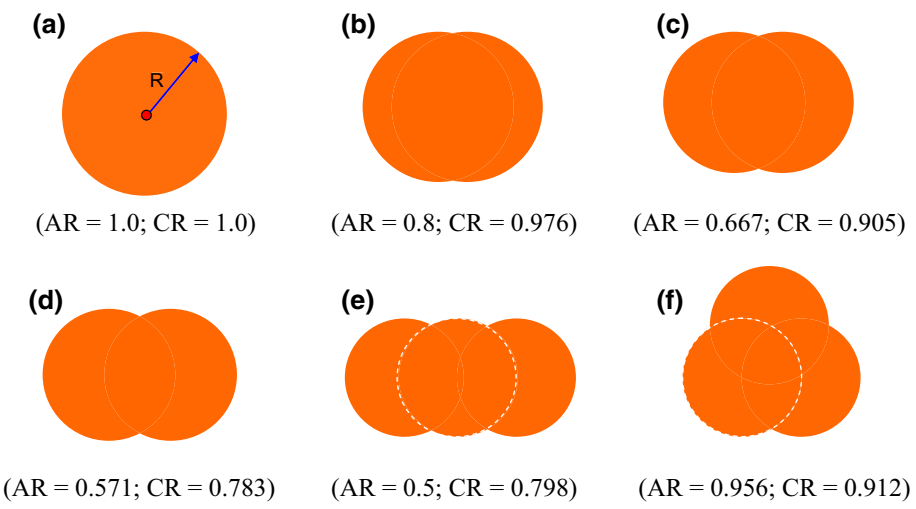

Fig. 1 Description of particle shape, **a** Shape A (AR = 1.0; CR = 1.0), **b** Shape B (AR = 0.8; CR = 0.976), **c** Shape C (AR = 0.667; CR = 0.905), **d** Shape D (AR = 0.571; CR = 0.783), **e** Shape E (AR = 0.5; CR = 0.798), **f** Shape F (AR = 0.956; CR = 0.912)

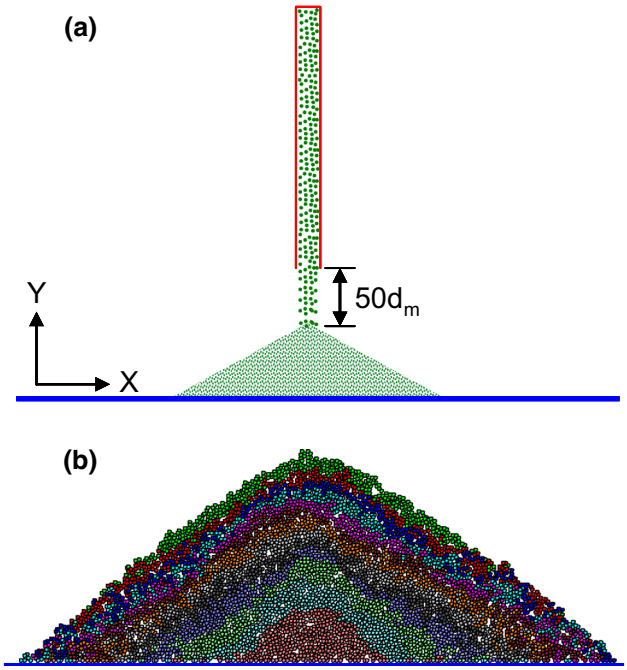

Fig. 2 **a** Schematic illustration of sandpile creation, and **b** a representative sandpile (Shape E), wherein d_m is the mean particle size

triangular-shaped particle (Fig. 1f). Except for the disk-shaped particle, we created the particles of other shapes by clumping two or three disks to form a rigid clump. This particle creation technique has been used by many other researchers [36–38]. It is worth mentioning that the term "particle" actually refers to "rigid clump" hereinafter. The particle sizes vary from 0.02 to 0.03 m. The particle size of a clumped particle is represented by the diameter of a circular particle having the same area as the clumped one. We employed the indices of aspect ratio (AR) and circularity (CR) to characterize the particle shape. The aspect ratio of a particle is defined to be the length ratio between the minor and major axes [39–42], and the circularity is referred to as the square of the perimeter ratio between this particle and an equivalent circular particle having the same area [43–45]. The values of shape parameters are given in Fig. 1. The particle density is 2.65 g/cm^3. The stiffness of bottom wall in both normal and tangential directions is 1.0×10^9 N/m. We used the linear elastic model to describe the contact behaviour between particles, and specified the normal and tangential stiffness of particles to be 1.0×10^9 N/m. We set the inter-particle and particle-wall friction coefficients to be 0.5. The local damping mechanism built in PFC2D is automatically activated, with the damping ratio set to be the default value 0.7.

As schematically shown in Fig. 2a, we constructed the sandpiles by pouring the particles which are physically dispersed in a narrow rectangular domain, onto a bottom wall. The narrow rectangular domain serves as a point source, with the dimension being $0.14 \times 1.6\,\mathrm{m}^2$. The floor is flat, with no micro-roughness, and the bottom layer of particles are not fixed in this study. Each sandpile contains about 2600 particles (see Fig. 2b). The angles of repose were estimated from the slopes of the left and right profiles.

The microstructures in granular media are usually quantified by the fabric tensor [46–50]. Kanatani [46] derived the fabric tensor of different ranks and used them to characterize the discrete distributional data. Topic et al. [48] described the microstructures by proposing the fabric tensor (i.e. Minkowski tensor) on the basis of the Voronoi tessellation of a particulate system. Rothenburg and Bathurst [49] used several continuous functions to characterize the angular distribution of microstructures and contact force network, with respect to the solid phase of granular packing:

Contact orientation:

$$E(\phi) = E_0\{1 + a_n \cos 2(\phi - \phi_n)\} \tag{1}$$

Contact normal force:

$$f(\phi) = f_0\left\{1 + a_f \cos 2(\phi - \phi_f)\right\} \tag{2}$$

Contact tangential force:

$$t(\phi) = -f_0 a_t \sin 2(\phi - \phi_t) \tag{3}$$

where E_0 represents the distribution probability density at an isotropic state and equals $1/2\pi$ for a 2D case; f_0 is the measure of mean contact normal force with the contacts in different directions given equal weight; ϕ refers to an interested direction angle; a_n, a_f and a_t give the anisotropy magnitudes respectively for contact orientation, contact normal force and contact tangential force, and ϕ_n, ϕ_f and ϕ_t denote the principal direction of anisotropy. In addition, one is able to define a probability density function similar to Eq. (1), to describe the angular distribution of particle orientations and thus have two similar indices: a_0 and ϕ_0, to characterize the fabric anisotropy of particle orientations.

3 Results and analysis

3.1 Effect of particle shape on angle of repose

Figure 3 plots the angles of repose for both left and right parts of sandpiles, respectively, against the aspect ratio AR and circularity CR. The angle of repose α is shown to decrease with the increase of AR and CR, implying that the more irregular the particle shape is, the larger the angle of repose is. This observation agrees with the experimental results of Ref. [45], which have been superimposed onto Fig. 3b.

Furthermore, we note that the experimental data of Ref. [45] are below the angles of repose for the cases of irregular shapes, but they are above those for the case of circular shape. This can be mainly ascribed to the reasons in two respects: (1) a kind of sand-sphere mixtures was used in the test of

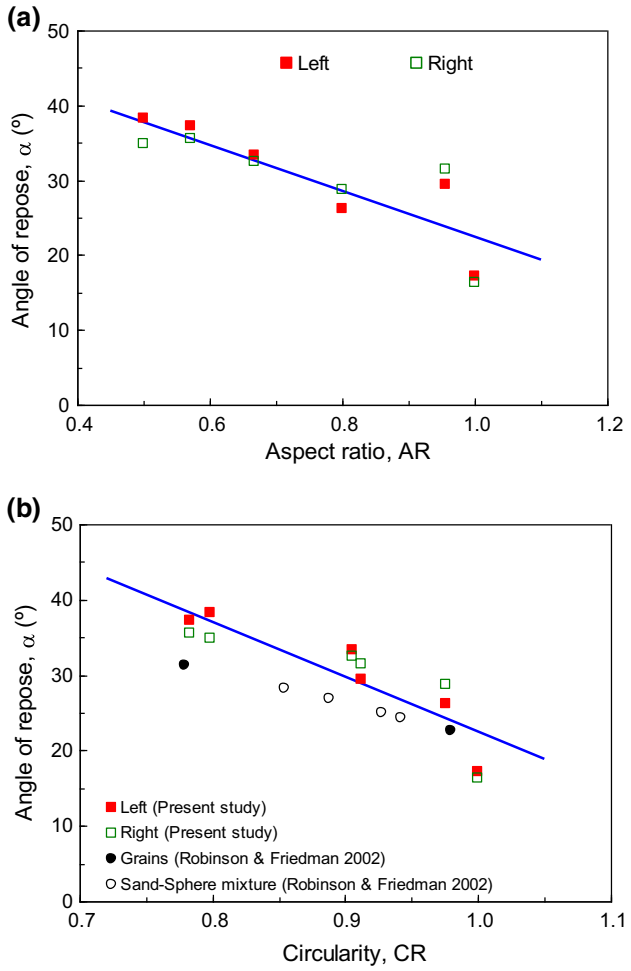

Fig. 3 The relations of angle of repose with the shape parameter: **a** α versus AR, **b** α versus CR

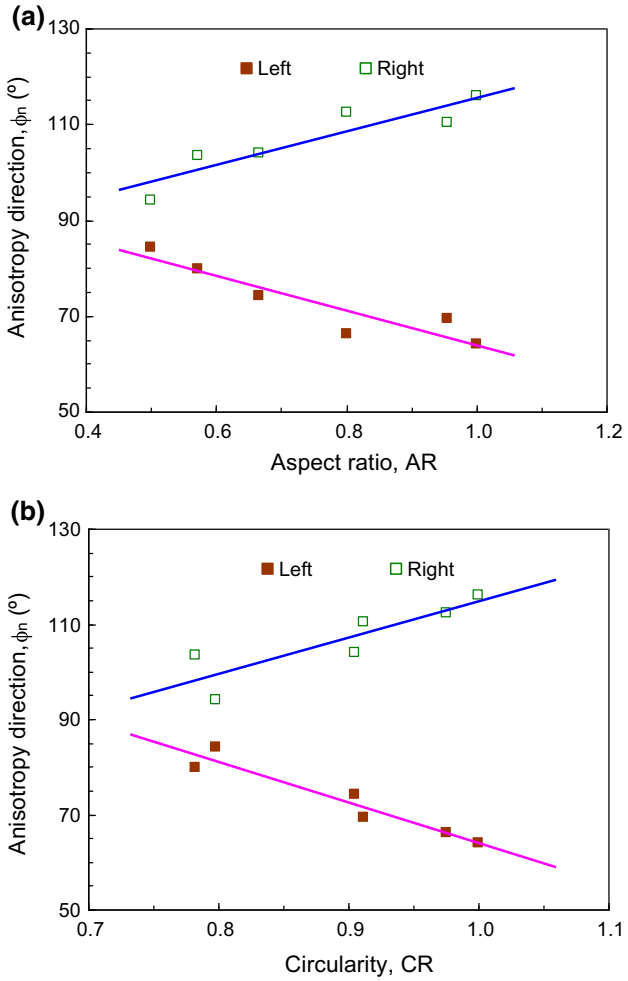

Fig. 4 The relations of fabric anisotropy of contact orientations with the shape parameter: **a** ϕ_n versus AR, **b** ϕ_n versus CR

Ref. [45], and the use of spherical particles may decrease the angle of repose due to the idealized particle shape; (2) the test setup is different from the numerical model in this study. In Ref. [45], an apparatus called as "Hele-Shaw cell" was used, in which the sandpile was bounded by two walls, including both horizontal and vertical boundaries, whereas there exists only the horizontal boundary wall in the current study. Nevertheless the boundary effect is an interesting issue requiring further study in the future. As far as rolling friction is concerned, it is assumed to be absent in this study. It is thought that the rolling friction would not play a primary role because the rolling friction is usually far less than the sliding friction for common granular materials.

3.2 Micromechanical analysis

3.2.1 Contact orientations

Figure 4 describes the relations between the fabric anisotropy of contact orientations and the shape parameter. We can find that the principal anisotropy direction ϕ_n for the left part increases as AR and CR increase, but it decreases with AR and CR for the right part, signifying that the principal anisotropy direction deviates increasingly away from the vertical direction as the shape parameter increases. We are able to see more clear evidences from the rose diagrams in Fig. 5, which exhibit the angular distribution of contact unit normal vectors in sandpiles.

We here plot the deviation angle $\Delta\phi_n$ of principal anisotropy direction relative to the vertical direction, against the angle of repose α (see Fig. 6). $\Delta\phi_n$ is shown to reduce with α. Interestingly, there seems to exist a linear relationship between $\Delta\phi_n$ and α, in which the summation of $\Delta\phi_n$ and α approximates to a constant 47°.

3.2.2 Particle orientations

Figure 7 presents the relations of the fabric anisotropy of particle orientations with the aspect ratio. The principal

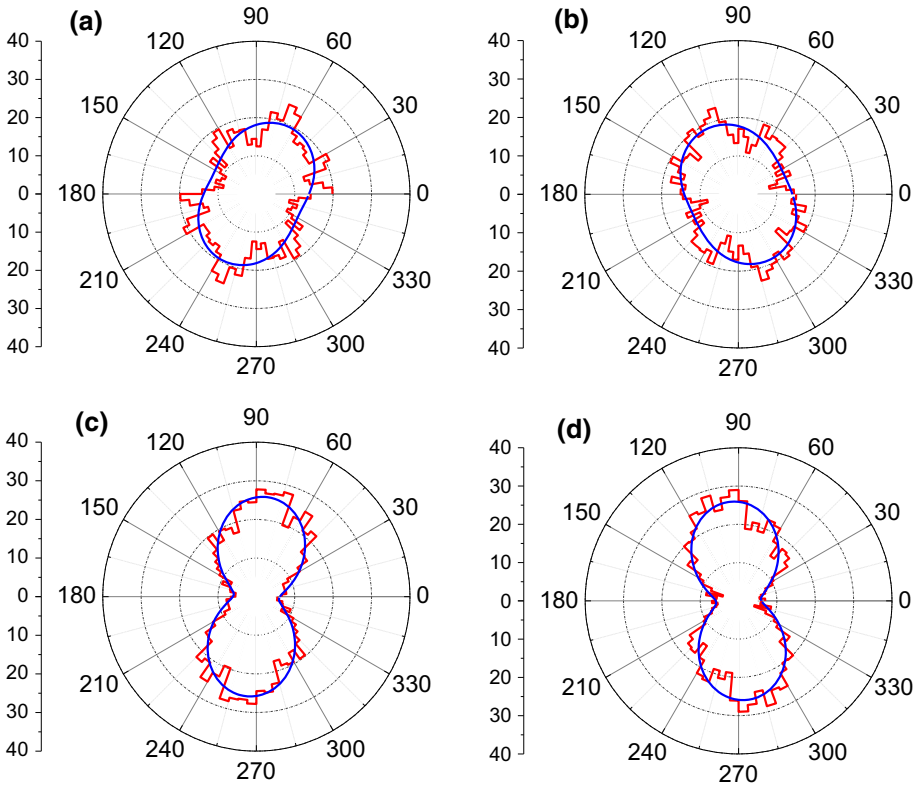

Fig. 5 The angular distribution probability densities (%) of contact orientation vectors: **a** *left part* of the case shape A (AR = 1.0, CR = 1.0), with $\phi_n = 64°$, **b** *right part* of the case shape A, with $\phi_n = 113°$, **c** *left part* of the case shape E (AR = 0.5, CR = 0.798), with $\phi_n = 84°$, and **d** *right part* of the case shape E, with $\phi_n = 94°$

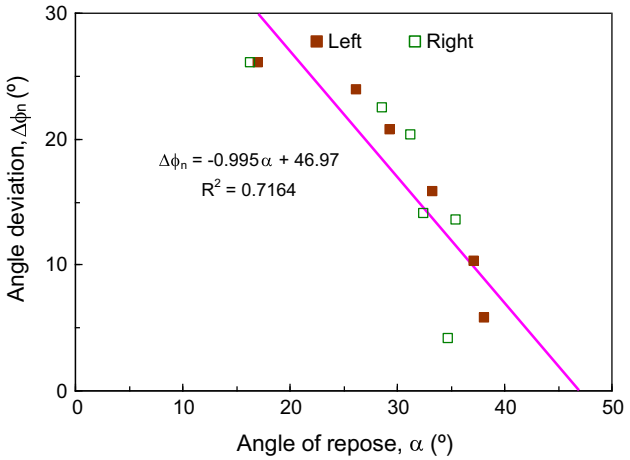

Fig. 6 The relationship between the deviation angle $\Delta\phi_n$ and the angle of repose α

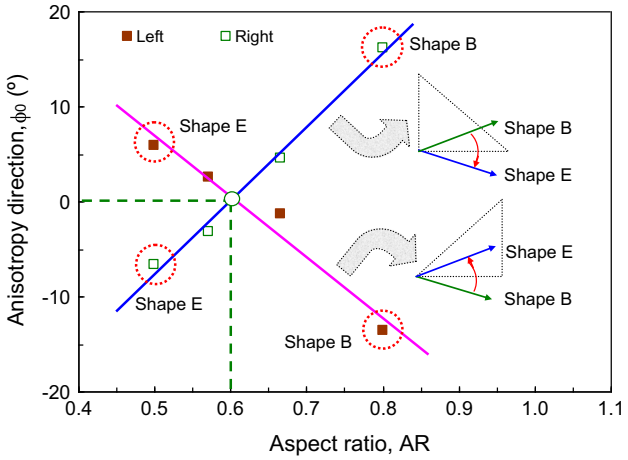

Fig. 7 The relations of fabric anisotropy of particle orientations with the aspect ratio: ϕ_0 versus AR

anisotropy direction ϕ_0 for the left part of the case shape B is a negative value which refers to a direction in the fourth quadrant of Cartesian coordinate system. As particle shape becomes more irregular, ϕ_0 increases with the decreasing AR, meaning that the principal anisotropy direction gradually rotates upward in the anti-clockwise direction, and ϕ_0 for the case shape E has even become a positive value denoting a direction in the first quadrant. The principal anisotropy direction for the right part undergoes a reverse variation trend. One is able to have closer scrutiny into the fabric anisotropy of particle orientations from the rose diagrams in Fig. 8.

Of great interest is the observation that the two best fit lines cross at the point (0.6, 0). We may infer that as AR varies, the two principle anisotropy directions respectively for the left and right parts of sandpile will reach a compromise state where these two half parts share the same principal anisotropy direction, and this characteristic state will take

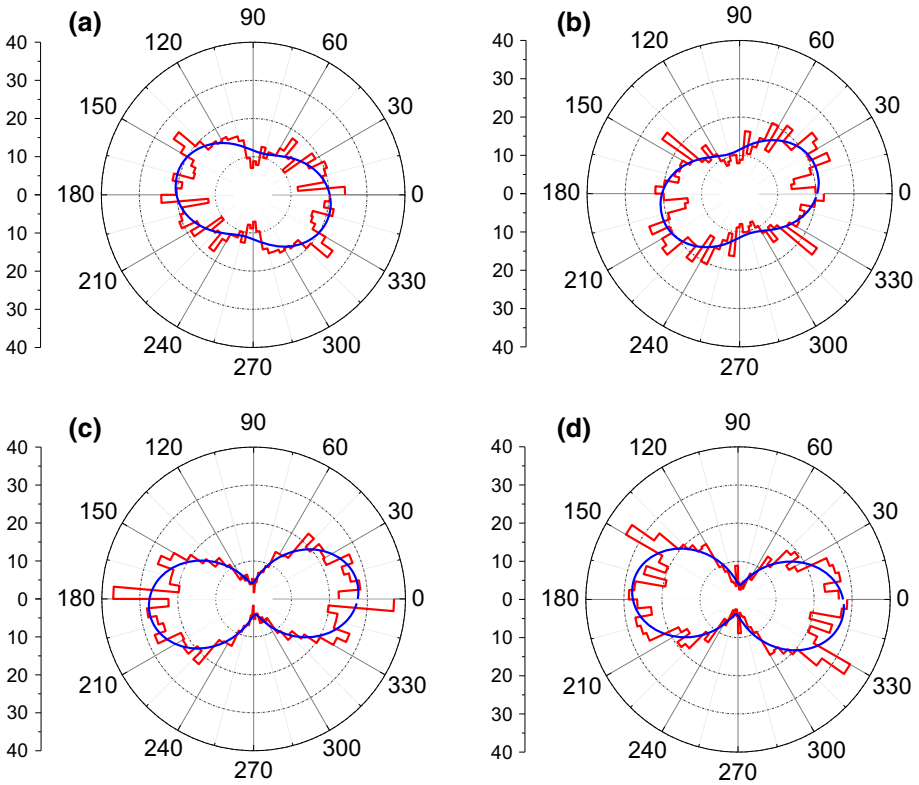

Fig. 8 The angular distribution probability densities (%) of particle orientation vectors: **a** *left part* of the case shape B (AR = 0.8), with $\phi_0 = -13.6°$, **b** *right part* of the case shape B, with $\phi_0 = 16.2°$, **c** *left part* of the case shape E (AR = 0.5), with $\phi_0 = 5.9°$, and **d** *right part* of the case shape E, with $\phi_0 = -6.7°$

place at AR = 0.6, with the common principal anisotropy direction being basically horizontal (i.e. $\phi_0 = 0°$).

Figure 9 gives the angular probability distributions of particle orientation vectors for the concerned four cases. We can see that the probabilities are the highest around $\theta = 0°$ and $\theta = 180°$, which indicates that the preferred particle orientations are around the horizontal direction. This finding agrees with the laboratory test finding of Ref. [8]. The observation also suggests that the granular flow along the sandpile surface does not exert a considerable impact on the orientations of particles, since the preferred particle orientations are not around the directions parallel to the sandpile profiles. Nevertheless one is still able to note that most particles are oriented beneath the directions of the left and right profiles of sandpiles, as the probabilities of particles being oriented within the two angle ranges $0° < \theta < \alpha$ and $180° - \alpha < \theta < 180°$, are comparatively large. For instance, the probability of particles orienting in these two angle ranges is around 60% for the case shape D ($\alpha = 36.4°$). As schematically illustrated in Fig. 10, the particles at "State I/III" (i.e. being oriented below the directions of the profiles of sandpile) are more stable than the ones at "State II/IV" (i.e. being oriented above the directions of the profiles of sandpile), and this may be the main reason why the preferred orientations of most particles are underneath the directions of the sandpile profiles.

3.2.3 Contact forces

We here plot in Fig. 11 the deviation angle $\Delta\phi_f$ formed between the principal anisotropy direction of contact normal forces and the vertical direction, against the angle of repose α, finding that $\Delta\phi_f$ appears to demonstrate a positive linear correlation with α, which is approximately expressed to be 0.67α. This indicates that the force anisotropy intensifies as the irregularity of particle shape is aggravated. We see from Fig. 12a that the weak force chains dominate the force network in quantity. The weak force chains are here defined to be the ones, in which the contact forces are less than the overall average contact force. As evidenced by Fig. 13, the occurrence probability of contacts with normal (tangential) contact forces $N_{cf}(T_{cf})$ being less than the average contact force $(N_{cf})_{\text{ave}}$ (e.g. $P_n \approx 0.68$ at the condition of $N_{cf}/(N_{cf})_{\text{ave}} < 1$), is relatively high, irrespective of the effect of particle shape. However, this does not mean that the weak force chains play a core role in the formation of arches in sandpiles. The strong force chains lie in the inner zone of sandpiles, propagating in general inclined to the middle axis line, and this has led to the formation of arches. Clearly the strong force chains play a vital role in the mobilization of arching effect.

Also, Fig. 12b shows that the principal stresses in the middle part of sandpiles are almost orientated in the horizontal

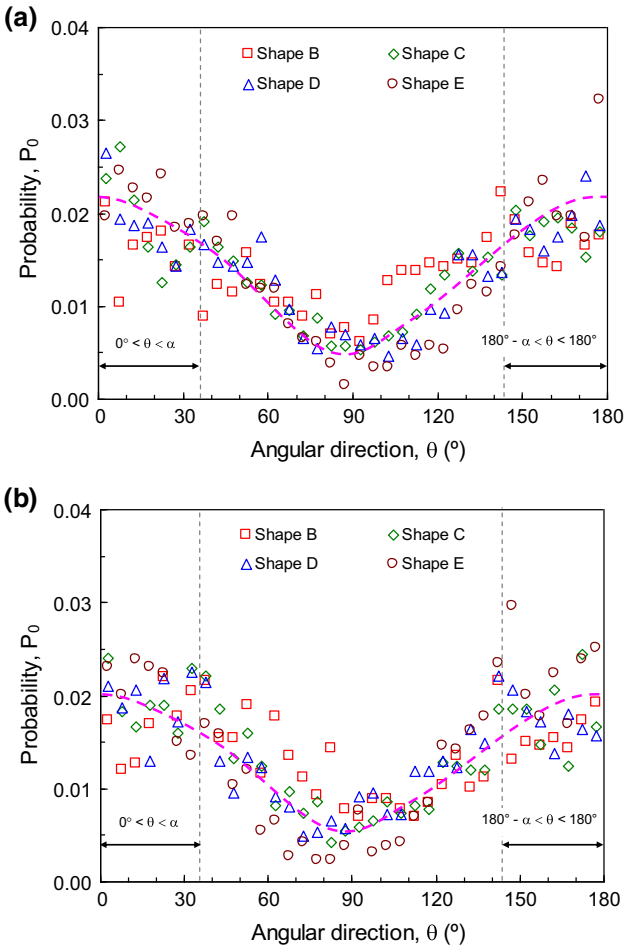

Fig. 9 The probabilities of the angular distribution of particle orientation vectors for **a** the *left part*, and **b** *right part* ($\alpha = 36.4°$ for the case shape D)

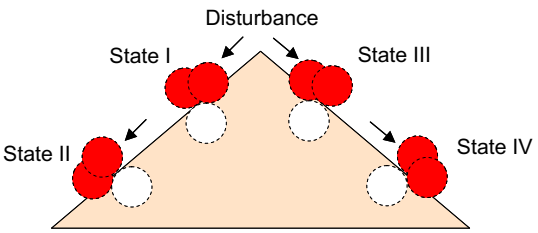

Fig. 10 Schematic illustration of the preferred orientations of particles

and vertical directions, and their orientations at the left and right sides have rotated. The rotation of principal stresses is evidently linked with the inclined propagation of strong force chains, and it is a manifestation of arching effect.

4 Discussion

In the following, we make a further discussion on the arching effect. We firstly plot in Fig. 14 the contact forces in the

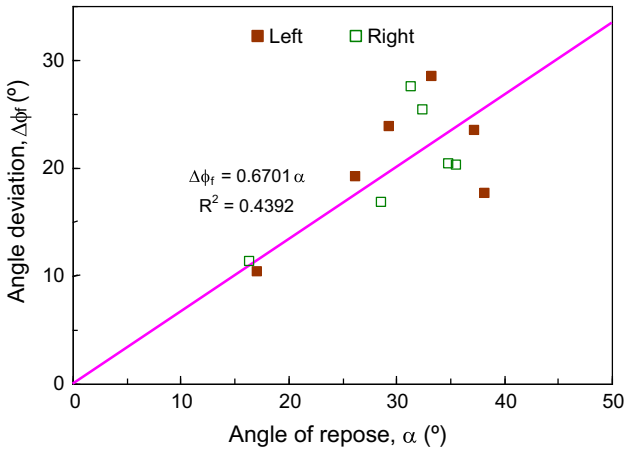

Fig. 11 The relationship between the deviation angle $\Delta\phi_f$ and the angle of repose α

main force chains ($N_{cf} > (N_{cf})_{\text{ave}}$) projected at various directions. The projected contact force at a given direction is a measurement of arching effect in this direction. We find that the projected contact forces for the left and right parts of sandpiles are symmetrical about the projection direction $\theta = 90°$ degrees. The peak projection force refers to the strongest arching phenomenon. Thus we can conclude from Fig. 14 that the strongest arching effect for the left part takes place in a directional zone of $\theta_p = 75° \sim 80°$ degrees, irrespective of the effect of particle shape, with that for the right part symmetrically occurring in the range of $\theta_p = 100° \sim 105°$ degrees.

In general the projected contact forces rely not only on the number and orientation of effective contacts in the force chains, but also on the force intensities. Therefore we attempt to relate the arching effect to both fabric and force anisotropy, by plotting in Fig. 15 the angle θ_p as a function of the mean anisotropy direction $\phi_{\text{mean}} (= (\phi_f + \phi_n)/2)$ which refers to the intermediate direction of the two principal anisotropy directions respectively for the contact orientations and contact normal forces. Although the scattering of data points is not obvious, we note that they almost fall on or beside the line $\theta_p = \theta_{\text{mean}}$. This observation implies that the strongest arching effect almost occurs in the mean anisotropy direction. This interesting finding may shed some light on the relationship between the arching effect and the fabric anisotropy.

5 Conclusions

We have probed the origin of angle of repose by conducting a DEM simulation of sandpile formation in consideration of the effect of particle shape. We have revealed the relationships between the angle of repose and the fabric anisotropy:

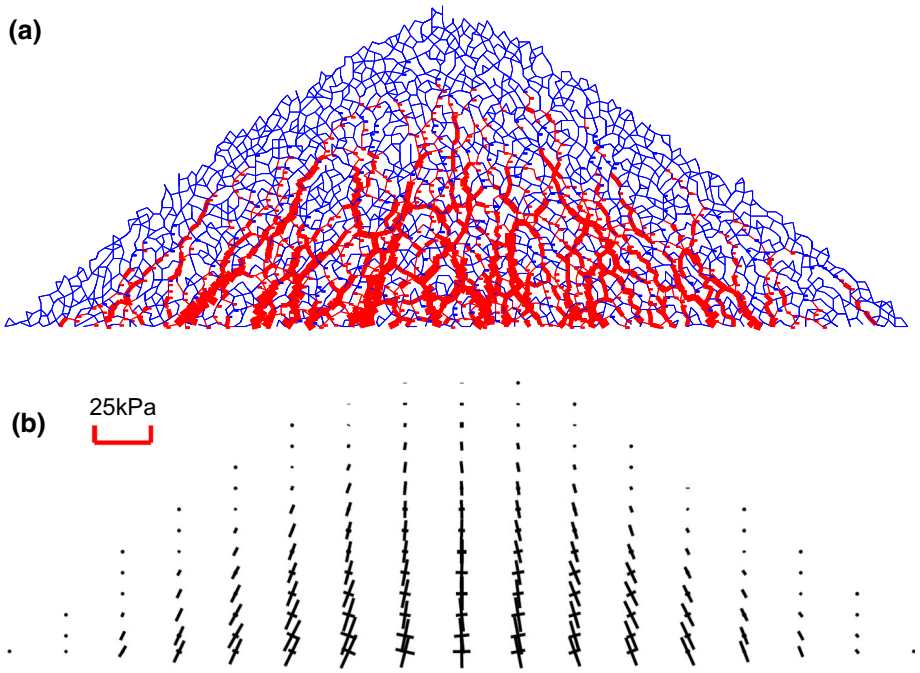

Fig. 12 Force chains and principle stress field (shape D): **a** force chains (*red* and *blue* represent respectively the strong and weak force chains), and **b** principle stress field (color figure online)

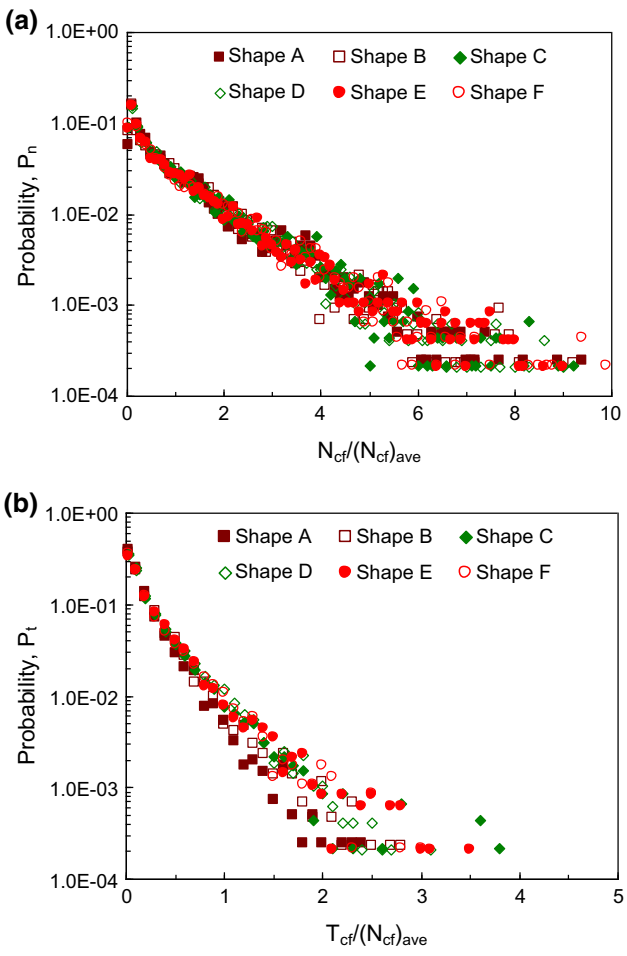

Fig. 13 The occurrence probability of contacts at different force magnitude levels: **a** contact normal force, **b** contact tangential force

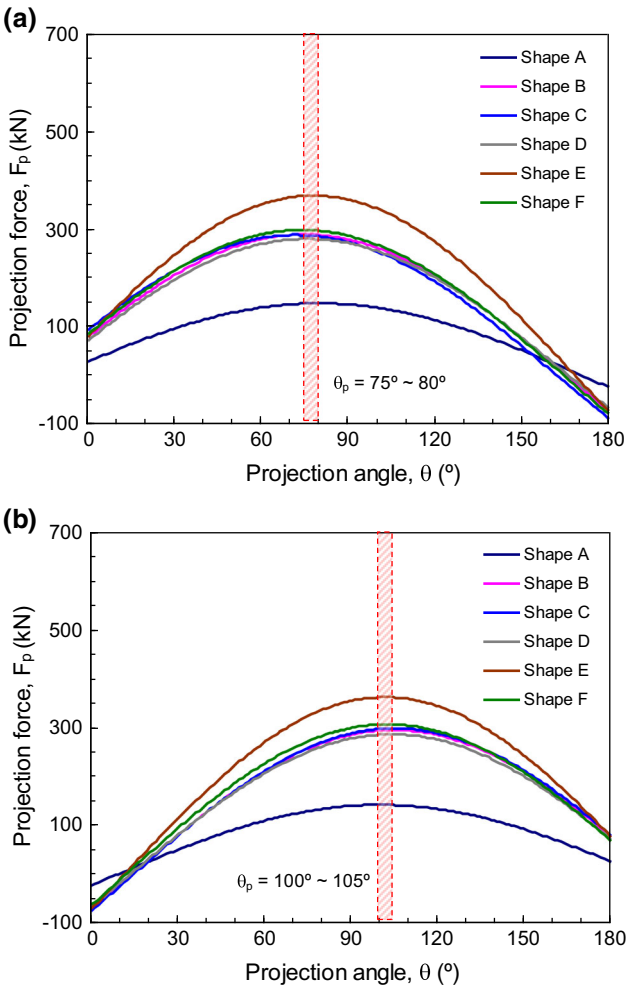

Fig. 14 Projection of the contact forces in the main force chains in the **a** *left part*, and **b** *right part* of sandpiles

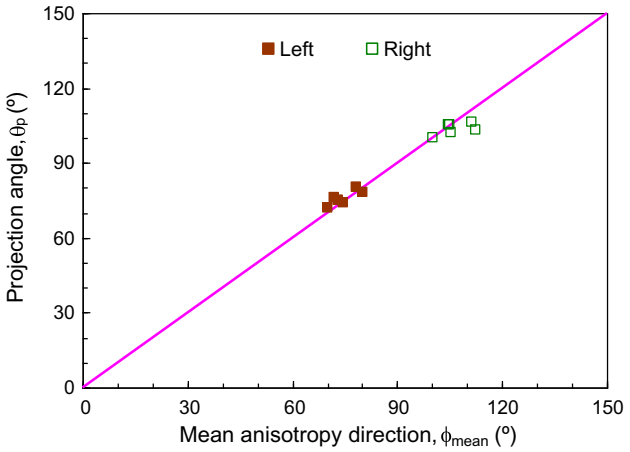

Fig. 15 The correlation of θ_p with the micromechanical index ϕ_{mean}

(1) the summation of the angle of repose α with the deviation angle $\Delta\phi_n$ is nearly a constant; (2) the deviation angle $\Delta\phi_f$ exhibits a positive correlation with the angle of repose, which is approximately expressed to be $\Delta\phi_f = 0.67\alpha$ in this study. We have interestingly noticed that the principal anisotropy directions of particle orientations undergo rotations as AR varies. Also we have identified a characteristic aspect ratio AR = 0.6, at which the principal anisotropy directions of particle orientations in the left and right parts of sandpiles tend to lie in the horizontal direction. By examining the projected contact forces of main force chains, we have found that the strongest arching effect takes place in the two symmetrical directional zones $\theta_p = 75^\circ \sim 80^\circ$ degrees (left part) and $\theta_p = 100^\circ \sim 105^\circ$ degrees (right part), and that the directional angle θ_p is basically the intermediate direction of the two principal anisotropy directions respectively for the contact orientations and contact normal forces.

Lastly it should be mentioned that we constructed the sandpiles from a point source and in a wedge sequence, and the results and conclusions may be only valid for this situation.

Acknowledgements We thank the financial support provided by the National Natural Science Foundation of China (No. 51209237; 51428901) and the Fundamental Research Funds for the Central Universities (No. 13lgpy05).

Compliance with ethical standards

Conflict of interest We here declare that we have no financial and personal relationships with other people or organizations which can inappropriately influence the work presented in this manuscript, and that there is no professional or other personal interest of any nature or kind in any product, service and/or company which could be construed as influencing the position presented in, or the review of, this manuscript.

References

1. Brockbank, B., Huntley, J.M., Ball, R.C.: Contact force distribution in beneath a three-dimensional granular pile. J. Phys. II Fr. **7**, 1521–1532 (1997)
2. Vanel, L., Howell, D.W., Clark, D., Behringer, R.P., Clément, E.: Memories in sand: experimental tests of construction history on stress distributions under sandpiles. Phys. Rev. E. **60**, R5040–R5043 (1999)
3. Mueggenburg, N.W., Jaeger, H.M., Nagel, S.R.: Stress transmission through three-dimensional ordered granular arrays. Phys. Rev. E. **66**, 031304 (2002)
4. Atman, A.P.F., Brunet, P., Geng, J., Reydellet, G., Claudin, P., Behringer, R.P., Clément, E.: From the stress response function (back) to the sand pile "dip". Eur. Phys. J. E **13**, 93–100 (2005)
5. Liu, Y.Y.: Arching effect in confined granular materials. Ph.D. Dissertation, Department of Civil Engineering, The University of Hong Kong, Hong Kong (2010)
6. Geng, J., Longhi, E., Behringer, R.P., Howell, D.W.: Memory in two-dimensional heap experiments. Phys. Rev. E **64**, 060301 (2001)
7. Zuiguel, L., Mullin, T., Rotter, J.M.: The effect of particle shape on the stress dip under a sandpile. Phys. Rev. Lett. **98**, 028001 (2007)
8. Zuiguel, L., Mullin, T.: The role of particle shape on the stress distribution in a sandpile. Proc. R. Soc. A **464**, 99–116 (2008)
9. Zhang, L., Cai, S., Hu, Z., Zhang, J.: A comparison between bridges and force-chains in photoelastic disk packing. Soft Matter **10**, 109–114 (2014)
10. Bouchaud, J.P., Claudin, P., Clément, E., Otto, M., Reydellet, G.: The stress response function in granular materials. C. R. Phys. **3**, 141–151 (2002)
11. Liu, C.H., Nagel, S.R., Schecter, D.A., Coppersmith, S.N., Majumda, S., Narayan, O., Witten, T.A.: Force fluctuation in beads packs. Science **269**, 513–515 (1995)
12. Coppersmith, S.N., Liu, C.H., Majumda, S., Narayan, O., Witten, T.A.: Model for force fluctuation in bead packs. Phys. Rev. E. **53**, 4673–4685 (1996)
13. Howell, D., Behringer, R.P., Veje, C.: Stress fluctuations in a 2D granular Couette experiment: a continuous transition. Phys. Rev. Lett. **82**, 9241–9244 (1999)
14. Veje, C., Howell, D., Behringer, R.P.: Kinematics of a two-dimensional granular Couette experiment at the transition to shearing. Phys. Rev. E. **59**, 739–745 (1999)
15. Bouchaud, J.P., Cates, M.E., Claudin, P.: Stress distribution in granular media and nonlinear wave equation. J. Phys. I Fr. **5**, 639–656 (1995)
16. Wittmer, J.P., Claudin, P., Cates, M.E., Bouchaud, J.P.: An explanation for the central stress minimum in sand piles. Nature **382**, 336–338 (1996)
17. Wittmer, J.P., Cates, M.E., Claudin, P.: Stress propagation and arching in sandpiles. J. Phys. I Fr. **7**, 39–80 (1997)
18. Alonso, J.J., Hovi, J.P., Herrmann, H.J.: Lattice model for the calculation of the angle repose from microscopic grain properties. Phys. Rev. E. **58**, 672–680 (1998)
19. Herrmann, H.J.: Statistical models for granular materials. Phys. A **263**, 51–62 (1999)
20. Hill, J.M., Cox, G.M.: The force distribution at the base ofsandpiles. Developments in Theoretical Geomechanics, The John Booker Memorial Symposium, 43–61 (2000)
21. Pipatpongsa, T., Heng, S., Lizuka, A., Ohta, H.: Statics of loose triangular embankment under Nadai's sand hill analogy. J. Mech. Phys. Solids **58**, 1506–1523 (2010)
22. Aranson, I.S., Tsimring, L.S.: Patterns and collective behavior in granular media: theoretical concepts. Rev. Mod. Phys. **78**, 641–692 (2006)

23. Duran, J.: Sand, Powders, and Grains: An Introduction to the Physics of Granular Materials. Springer, New York (1999)
24. Jaeger, H.M., Nagel, S.R., Behringer, R.P.: Granular solids, liquids, and gases. Rev. Mod. Phys. **68**, 1259–1273 (1996)
25. Lee, J., Herrmann, H.J.: Angle of repose and angle of marginal stability: molecular dynamics of granular particles. J. Phys. A: Math. Gen. **26**, 373–383 (1993)
26. Luding, S.: Stress distribution in static two-dimensional granular model media in the absence of friction. Phys. Rev. E **55**, 4720–4729 (1997)
27. Zhou, Y.C., Xu, B.H., Yu, A.B., Zulli, P.: Numerical investigation of the angle of repose of monosized spheres. Phys. Rev. E **64**, 021301 (2001)
28. Goldenberg, C., Goldhirsch, I.: Friction enhances elasticity in granular solids. Nature **435**, 188–191 (2005)
29. Liffman, K., Nguyen, M., Metcalfe, G., Cleary, P.: Forces in piles of granular materials: an analytic and 3D DEM study. Granul. Matter **3**, 165–176 (2001)
30. Li, Y., Xu, Y., Thornton, C.: A comparison of discrete element method simulations and experiments for 'sandpile' composed of spherical particles. Powder Technol. **160**, 219–228 (2005)
31. Matuttis, H.G.: Simulation of the pressure distribution under a two-dimensional heap of polygonal particles. Granul. Matter **1**, 83–91 (1998)
32. Matuttis, H.G., Luding, S., Herrmann, H.J.: Discrete element simulations of dense packing and heaps made of spherical and non-spherical particles. Powder Technol. **109**, 278–292 (2000)
33. Zhou, C., Ooi, J.Y.: Numerical investigation of progressive development of granular pile with spherical and non-spherical particles. Mech. Mater. **41**, 707–714 (2009)
34. Zhou, Z.Y., Zou, R.P., Pinson, D., Yu, A.B.: Angle of repose and stress distribution of sandpiles formed with ellipsoidal particles. Granul. Matter **16**, 695–709 (2014)
35. PFC2D: User's manual for PFC2D. Itasca Consulting Group Inc, Minneapolis (2005)
36. Li, X., Yu, H.-S.: Numerical investigation of granular material behaviour under rotational shear. Géotechnique **60**, 381–394 (2010)
37. Yang, Z.X., Yang, J., Wang, L.Z.: Micro-scale modeling of anisotropy effects on undrained behavior of granular soil. Granul. Matter **15**, 557–572 (2013)
38. Dai, B.B., Yang, J., Luo, X.D.: A numerical analysis of the shear behavior of granular soil with fines. Particuology **21**, 160–172 (2015)
39. Cavarretta, I., Coop, M., O'Sullivan, C.: The influence of particle characteristics on the behaviour of coarse grained soils. Géotechnique **60**, 413–423 (2010)
40. Yang, J., Wei, L.M.: Collapse of loose sand with the addition of fines: the role of particle shape. Géotechnique **62**, 1111–1125 (2012)
41. Yang, J., Luo, X.D.: Exploring the relationship between critical state and particle shape for granular materials. J. Mech. Phys. Solids **84**, 196–213 (2015)
42. Yang, Y., Wang, J.F., Cheng, Y.M.: Quantified evaluation of particle shape effects from micro-to-macro for non-convex grains. Particuology **25**, 23–35 (2015)
43. Wadell, H.: Volume, shape, and roundness of rock particles. J. Geol. **40**, 443–451 (1932)
44. Wadell, H.: Volume, shape, and roundness of quartz particles. J. Geol. **43**, 250–280 (1935)
45. Robinson, D.A., Friedman, S.P.: Observations of the effects of particle shape and particle size distribution on avalanching of granular media. Phys. A **311**, 97–110 (2002)
46. Kanatani, K.: Distribution of directional data and fabric tensors. Int. J. Eng. Sci. **22**, 149–164 (1984)
47. Satake, M.: Fabric tensor in granular materials. In: IUTAM Symposium onDeformation and Failure of Granular Materials, Delft, 63-68 (1982)
48. Topic, N., Schaller, F.M., Schröder-Turk, G.E., Pöschel, T.: The microscopic structure of mono-disperse granular heaps and sediments of particles on inclined surfaces. Soft Matter **12**, 3184–3188 (2016)
49. Rothenburg, L., Bathurst, R.J.: Analytical study of induced anisotropy in idealized granular materials. Géotechnique **39**, 601–614 (1989)
50. Oda, M.: Fabric tensor and its geometrical meaning. In: Oda, M., Iwashita, K. (eds.) Mechanics of Granular Materials: An introduction, pp. 27–35. A.A. Balkema, Rotterdam (1999)